

Formation of Electronically Excited Fragments Resulting from Collisions of He(2^3S) Atoms with CCl_4 and Related Chloromethanes

Ikuo Tokue,* Masaaki Kobayashi, Takeyuki Kudo, and Katsuyoshi Yamasaki

Department of Chemistry, Faculty of Science, Niigata University, Ikarashi, Niigata 950-2181

(Received June 29, 2001)

The photoemissions from fragments produced by collisions of He(2^3S) atoms with $CHCl_3$, CCl_2F_2, CCl_3F, CCl_4, and $CBrCl_3$ have been studied in the collision energy range of 120–210 meV using a crossed beam. The Cl_2(D′–A′) band is predominant for CCl_4 and $CBrCl_3$, while the A–X and B–X bands of CF are intense for CCl_2F_2 and CCl_3F. The sum of the emission cross sections (σ_{em}) for several systems of neutral fragments in the 190–600 nm region was estimated to be in the (0.3–1.2) $\times$ 10^{-20} m^2 range for these chloromethanes at a collision energy of 150 meV. The dependences of σ_{em}'s for the Cl_2(D′–A′) band from $CHCl_3$ and CCl_4 on the collision energy are either nearly zero or slightly negative. The sum of σ_{em}'s for Cl_2 and other ion-pair bands reveals a fairly good correlation with the electron affinity of the targets. These results support the harpoon mechanism for the formation of Cl_2(D′) from the He(2^3S) + chloromethanes reactions.

The formations of electronically excited states resulting from the collisions of metastable atoms (A^*) and simple molecules have been extensively studied by optical spectroscopy. In these studies, we determine the emission rate constants or emission cross sections (σ_{em}) of electronically excited states and their internal energy distributions for understanding the dissociation processes and interactions between A^* and simple molecules.[1] The interaction of A^*, especially Ar($^3P_2$), Kr($^3P_2$), and Xe($^3P_2$), with halogen-containing molecules (RX) has received great interest in connection with the formation of excited states of AX, which can be utilized as an excimer laser. Most aspects of the A^* and RX reactions can be explained by the harpoon model in which the exit channel state of $AX^* + R$ is produced via the ion-pair intermediate $A^+\cdots RX^-$.[2] On the other hand, the formation of the HeX^* state is not known in the reactions of He(2^3S) with RX, while emissions from several fragments were observed in the reactions of He(2^3S) with chloromethanes[3–5] and chlorofluoromethanes.[6–7] Tsuji et al.[7] studied the dissociative excitation of CF_nCl_{4-n} (n = 0–4) by collisions with Ar and He active species, and determined the emission rate constants for several reactions at thermal energy. Li et al.[5] measured the formation rate constants of excited states for H, CH, and CCl fragments produced by the collisions of He(2^3S) with CH_nCl_{4-n} (n = 1–4) under the beam conditions and discussed the energy-partitioning process based on an analysis concerning the rotational and vibrational distributions for the A and B states of the CH radical. Unfortunately, Li et al. did not mention Cl_2^* emission, which seems to appear in the spectrum observed from $CHCl_3$ (Fig. 1 in Ref. 5); it is uncertain whether the Cl_2^* emission is directly produced from $CHCl_3$ or not. Thus, there has been only a small amount of information about the formation mechanism of neutral fragments resulting from the reaction of He(2^3S) with chloromethanes, especially at higher collision energies. These dissociation processes are expected to play an important role in CCl_nF_{4-n}/He discharges, which are frequently used in the plasma etching of several materials. At any rate, formation of neutral fragments resulting from the reaction of He(2^3S) with chloromethanes can be explained by either the harpoon model or an electron exchange model; the initial step for the latter model is similar to the model applied to Penning ionization.[8]

When the excitation energy of He(2^3S) exceeds the lowest ionization potential of target molecules (M), several types of chemi-ionization can occurs; especially the Penning ionization become dominant:

$$He(2^3S) + M \rightarrow He + M^+ + e^-.$$

The Penning ionization of He(2^3S) atoms with simple molecules was studied extensively by various types of experiments,[9] and the interactions of the entrance and exit channels and ionization mechanisms have thus been well characterized based on the electron exchange model.[8] The situation is more complicated for the formation of neutral fragments resulting from reactions of He(2^3S) with simple molecules. The neutral fragments will be produced through the predissociation of superexcited states;[10] excitation to the superexcited state can be interpreted in terms of the electron-exchange mechanism: a valence electron of the target falls into the 1s hole orbital of He(2^3S) and simultaneously the 2s electron of He(2^3S) rises to one of the unoccupied orbitals of the target. The neutral dissociation of superexcited states thus produced generally competes with autoionization, since the electronic energy of He(2^3S) is usually higher than the ionization potentials of the valence electrons of simple molecules.

In the present study, photoemissions from excited fragments produced by collisions of He(2^3S) with $CHCl_3$, CCl_2F_2, CCl_3F, CCl_4, and $CBrCl_3$ have been observed using a crossed beam for understanding of dissociation mechanism. Photoemission cross sections (σ_{em}) of several neutral fragments and their dependences on the relative collision energy have been measured. The formation processes of these excited fragments are

discussed based on the correlation of the σ_{em} values with the electron affinity of the target molecules and the interaction potentials of He(2^3S) with the target molecules ($CHCl_3$ and CCl_4) calculated by ab initio molecular orbital methods.

Experimental

The apparatus and experimental details concerning the fluorescence measurement were reported previously.[11,12] In brief, He(2^3S, 2^1S) atoms are produced with a nozzle discharge source[13] and skimmed into a collision chamber; the singlet component of the total He* flux was estimated to be about 10%. Target gases flowed out to the collision chamber, forming an effusive molecular beam through a multicapillary array. Under typical stable operating conditions, the discharge current was 10–20 mA, the voltage was 500–850 V, and the pressure of the residual gas at the collision chamber measured by an ionization vacuum gauge was less than 2.7 mPa. Samples of $CHCl_3$, CCl_2F_2, CCl_3F, CCl_4, and $CBrCl_3$ obtained commercially were used after degassing.

The velocity distributions of the He* beam were measured with a separate apparatus equipped with a similar He* beam source.[12] The root-mean-square velocity (v_A) of the He* beam was found to depend only on the discharge power at the beam source. The collision energy dependence of σ_{em} was obtained by converting the function of v_A into that of the relative collision energy (E_R) with the relation between E_R and the reduced mass (μ) of the He + target system,

$$E_R = \mu(v_A{}^2 + 3kT/m)/2, \quad (1)$$

where T is the temperature (300 K) and m is the mass of the target molecule. In the fluorescence measurement, we did not use the velocity-selected He* beam because of the weak fluorescence intensity. Thus, applying the fact that v_A increases with the discharge power, we controlled the kinetic energy of the He* beam by varying the discharge power. The kinetic energy distribution of the He* beam was estimated to be 40 meV (hwhm) at E_R values of 120 meV and 80 meV at 200 meV. It should be mentioned that the σ_{em} values were measured with a relatively broad collision energy distribution.

The fluorescence resulting from the collision of He(2^3S) atoms with the target molecules was observed in a direction perpendicular to both the molecular and He* beams. In the present study, the σ_{em} for the fluorescence produced by collisions of He(2^3S) was evaluated by comparing its emission intensity with that of the $N_2{}^+(B^2\Sigma_u{}^+ - X^2\Sigma_g{}^+)$ band produced by the Penning ionization,[12]

$$He(2^3S) + N_2 \rightarrow N_2{}^+(B^2\Sigma_u^+) + He + e^-. \quad (2)$$

We adopted a σ_{em} value of $(3.2 \pm 0.3) \times 10^{-20}$ m^2 for reaction 2 at an E_R of 140 meV; this value was estimated from Fig. 5 in Ref. 14. The total emission intensity of the $N_2{}^+$(B–X) system was derived from the intensities of the 0–0 and 1–0 bands by using the scaling factors calculated by Comes and Speier.[15] The density and spatial distribution of N_2 and the target molecules at the collision region were calibrated from the pressure measured with an MKS Baratron.

Calculations

In order to discuss the observed results concerning the collision energy dependence of the σ_{em} values, the interaction-potential curves for a He(2^3S) atom approaching a carbon atom or a chlorine atom along several directions were calculated for $CHCl_3$ and CCl_4 using ab initio molecular orbital (MO) methods. Since there are difficulties associated with calculating the excited states and a well-known resemblance between He(2^3S) and Li(2^2S),[9,16] in the present study a Li(2^2S) atom was used in place of He(2^3S).[13,17]

The interaction potentials between a Li(2^2S) atom and $CHCl_3$ or CCl_4 were calculated using the Gaussian 94 program package[18] in the Møller–Plesset perturbation method (MP2) with the frozen-core approximation. The standard 6-31++G** basis set was used.

Results and Discussion

Emission Spectra. Figure 1 shows the emission spectra produced by collisions of He(2^3S) with the target molecules. The 278-nm peak, which was observed from all parents, is the well-known CCl ($A^2\Delta$–$X^2\Pi$) system.[19] The broad band in the 190–270 nm region with a peak at 257 nm is assigned to the Cl_2(D′2g–A′$^3\Pi_{2u}$) system;[20,21] the D′ state is an ion-pair state correlating with the $Cl^+(^3P) + Cl^-(^1S)$ state. The emission spectrum from $CHCl_3$ is basically similar to that reported by Li et al.,[5] except that the Cl_2(D′–A′) band is more intense in the present study. The features in the spectra from CCl_2F_2, CCl_3F, and CCl_4 are similar to those measured at thermal energy.[7] The Cl_2(D′–A′) band from $CHCl_3$, CCl_4, and $CBrCl_3$ is intense, while this band from CCl_3F becomes weak and almost disappears for CCl_2F_2. It is concluded that the Cl_2* emission is produced by a single collision of He(2^3S) with target molecules under the present crossed-beam conditions. In the electron-impact dissociation of chloromethanes, Tokue et al.[22] observed a similar Cl_2* emission, which is assigned as the D′–A′ system, and concluded that Cl_2(D′) is directly produced by single collisions of incident electrons with target molecules. Although we did not find available spectroscopic data, the 306 and 333 nm bands observed from $CHCl_3$, CCl_3F, CCl_4, and $CBrCl_3$ are attributed to Cl_2* emissions.[22]

For $CBrCl_3$, a broad peak at 314 nm is assigned to the BrCl(D′2–A′$^3\Pi_2$) system and the 375 nm band is attributable to a BrCl* emission.[22] For CCl_2F_2 and CCl_3F, the several peaks in the 190–250 nm region are assigned to the CF($B^2\Delta$–$X^2\Pi$) and CF($A^2\Sigma^+$–$X^2\Pi$) bands,[23] and a peak at 285 nm is ascribable to the ClF(D′2–A′$^3\Pi_2$) system.[22] No fluorescence from ions was identified for all parents.

σ_{em}'s and Dissociation Processes. Table 1 lists σ_{em}'s for several excited fragments produced by collisions of He(2^3S) with chloromethanes at an E_R of 150 meV. The main cause for the error attached to the σ_{em} values is the uncertainty (10%) in the σ_{em} value for reference reaction 2, while the experimental error is estimated to be 4%–12%, except for the emissions overlapping with other bands. The experimental error includes the fluctuation of the He* flux, the uncertainty in the relative sensitivity of the photon-detection system, and the uncertainty in the relative gas density. The He(2^1S) component in the He* beam may affect the σ_{em} values. There is very little quantitative data on the partial cross section for the He(2^1S) reactions with simple molecules. Nevertheless, the total chemiionization cross sections for He(2^1S) with simple molecules have been carefully compared with those for He(2^3S) using the crossed-beam technique;[25] the ratios of the cross section for

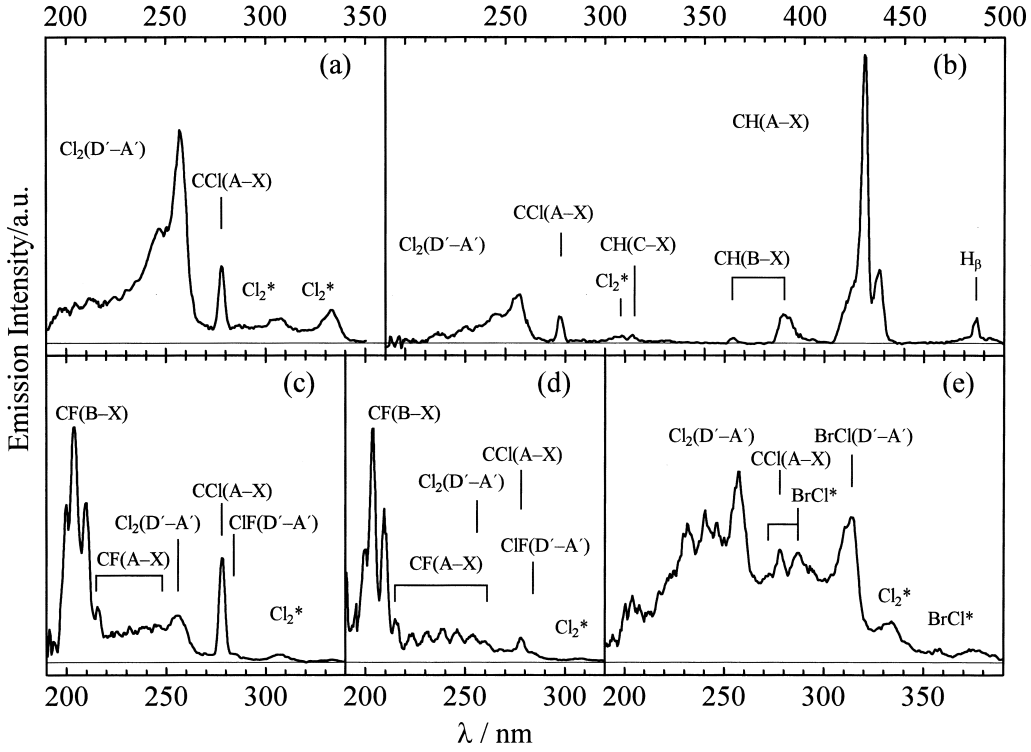

Fig. 1. Typical emission spectra resulting from collisions of He(2^3S) with (a) CCl_4, (b) $CHCl_3$, (c) CCl_3F, (d) CCl_2F_2, and (e) $CBrCl_3$ measured at E_R of 150 meV with the optical resolution of 3.3 nm (fwhm); the optical sensitivity is calibrated.

Table 1. σ_{em} Values of Several Emissions Produced by Collision of He(2^3S) with Chloromethanes at E_R of 150 meV[a)]

Species		$\sigma_{em}/10^{-22}$ m^2				
	λ/nm	$CHCl_3$	CCl_2F_2	CCl_3F	CCl_4	$CBrCl_3$
CF($B^2\Delta$–$X^2\Pi$)	193–220		51.6(7.0)	25.5(3.0)		
CF($A^2\Sigma^+$–$X^2\Pi$)	200–274		30.8(7.6)	7.5(1.2)		
CCl($A^2\Delta$–$X^2\Pi$)	278	2.9(0.4)	1.2(0.5)	3.3(0.6)	1.4(0.2)	0.8(0.2)
CH($C^2\Sigma^+$–$X^2\Pi$)	314	0.6(0.3)				
CH($B^2\Sigma^-$–$X^2\Pi$)	360–402	10.1(1.5)				
CH($A^2\Delta$–$X^2\Pi$)	414–443	62(11)				
H_β	486	2.1(0.5)				
Cl_2($D'^3\Pi$–$A'^3\Pi$)	190–270	40.3(5.6)	2.7(0.8)	10.3(1.6)	24.3(6.7)	29.6(6.2)
Cl_2*	270–345	5.8(1.0)		2.1(0.6)	6.7(1.1)	3.2(0.6)
ClF($D'^3\Pi$–$A'^3\Pi$)	282–294		2.9(0.8)	0.47(0.13)		
BrCl*	230–390					30.5(3.5)
Total	196–600	123(13)	89(10)	49(4)	33(7)	64(7)

a) Numbers in parentheses represent the estimated uncertainties.

He(2^1S) to that for He(2^3S) are reported to be 0.9–1.8. In the present experiment, the contribution on the σ_{em} values from the He(2^1S) component were estimated to be within 10% on the assumption that the singlet-to-triplet ratio for each fragment is within two. The total σ_{em} values for these chloromethanes are in the (0.3–1.2) $\times$ 10^{-20} m^2 range, while the quenching cross section of He(2^3S) in 10^{-20} m^2 units was reported to be 84 for $CHCl_3$, 34 for CCl_2F_2, and 99 for CCl_4 at 300 K.[24] Thus, the total σ_{em}'s for these chloromethanes are roughly estimated to be 1% of the quenching cross section of He(2^3S); it is beyond doubt that the Penning ionization is the main quenching process, since the ionization cross sections for the collisions of He(2^3S) and simple molecules[25] are nearly equal to their quenching cross sections.[26]

The emitters produced from these chloromethanes can be classified into two groups: the first is the H, CH, CF, and CCl fragments, and the second is the ion-pair states of halogen and interhalogen molecules (ClF, Cl_2, and ClBr) newly formed after collision. For CCl_4 and $CBrCl_3$, a sum of the σ_{em}'s for the ion-pair states (σ^{i}_{em}) reaches above 90% of the total σ_{em} value. The fraction decreases to 26% for CCl_3F and 6% for CCl_2F_2. This indicates that the mechanism for the formation of the second group of emitters differs from that for the first group. The formation mechanism will be discussed in later. The trend for the fraction for the ion-pair states is in good agreement with the result measured at thermal energy.[7]

Table 2. Energetically Possible Reactions for Formation of $CCl(A^2\Delta)$ and $Cl_2(D'^3\Pi)$ from $CXCl_3$ (X = H, F, Cl, Br)

	ΔH/eV[a]			
Reaction[b]	$CHCl_3$	CCl_3F	CCl_4	$CBrCl_3$
(3) $CXCl_3 \rightarrow CCl(A) + XCl + Cl$	11.0	13.2	}12.0	11.5
(4) $CXCl_3 \rightarrow CCl(A) + Cl_2 + X$	13.0	13.3		11.3
(5) $CXCl_3 \rightarrow CCl(A) + X + 2Cl$	15.5	15.8	14.5	13.8
(6) $CXCl_3 \rightarrow Cl_2(D') + CXCl$	11.2†	9.4	10.0	unknown
(7) $CXCl_3 \rightarrow Cl_2(D') + CX + Cl$	15.2	13.3	}14.1	13.7†
(8) $CXCl_3 \rightarrow Cl_2(D') + CCl + X$	15.1	15.5		13.4
(9) $CXCl_3 \rightarrow Cl_2(D') + C + Cl + X$	18.7	19.0	17.0	17.0

a) Uncertainty is usually below 0.2 eV except the values indicated by the dagger (†).
b) The fragments without the electronic state are in the ground state.

Table 2 lists energetically possible dissociation processes by collisions of He(2^3S: 19.82 eV) leading to CCl(A) or $Cl_2(D')$, which appears from all targets. The threshold energies (ΔH) are calculated by using the enthalpies of formation for targets and related fragments[27] and the electronic energies of the excited states.[21,28,29] Process 5 seems to be predominant among energetically possible reactions leading to CCl(A), whereas processes 3 and 4 are probably minor, since they produce a newly bonded molecule despite large excess energies (6.5–8.8 eV). The Cl···Cl distances of chloromethanes are about 290 pm, which is nearly like the equilibrium bond length of the $Cl_2(D')$ state, 287.4 pm.[20] Thus, the formation of $Cl_2(D')$ can occur, whereas the formations of XCl and Cl_2 in the ground state such as processes 4 and 5 are probably difficult since the Cl···Cl or X···Cl distance in these chloromethanes is far larger than that of the ground state of Cl_2 or XCl.[28] Process 6 is probably negligible because of the large excess energy, while we cannot determine the relative importance of processes 7–9.

Collision Energy Dependence of σ_{em} and Interaction Potentials. The σ_{em}'s of the CCl(A–X) and $Cl_2(D'–A')$ emissions change largely with the target molecule, as shown in Table 1. This trend is very different from that obtained in the electron-impact dissociation: e.g. the σ_{em} of the CCl(A–X) band produced from the electron impact on $CXCl_3$ (X = H, F, Cl, Br) at an impact energy of 100 eV increases with the atomic number of X,[19] and the ratio of the intensity of the $Cl_2(D'–A')$ emission to that of the CCl(A–X) emission produced from CCl_4 is about four-times greater than the ratio obtained by the electron impact at 100 eV.[22] These results indicate that the mechanism for the formation of fragments produced from the He(2^3S) + chloromethanes reactions differs from that of the electron-impact dissociation. Decay channels in the collisions of He(2^3S) with target molecules are probably related to spatially extended orbitals and geometrically accessible parts of electron densities of individual molecular orbitals in target molecules (i.e. exterior electron density).[13]

In order to discuss the mechanism for the formation of excited fragments, it is effective to measure the dependence of σ_{em}'s for the fragments on the collision energy. If the attractive part of the interaction potential ($V^*(R)$) between He(2^3S) and M (target molecule) is described by

$$V^*(R) = -C_s/R^{-s}, \tag{10}$$

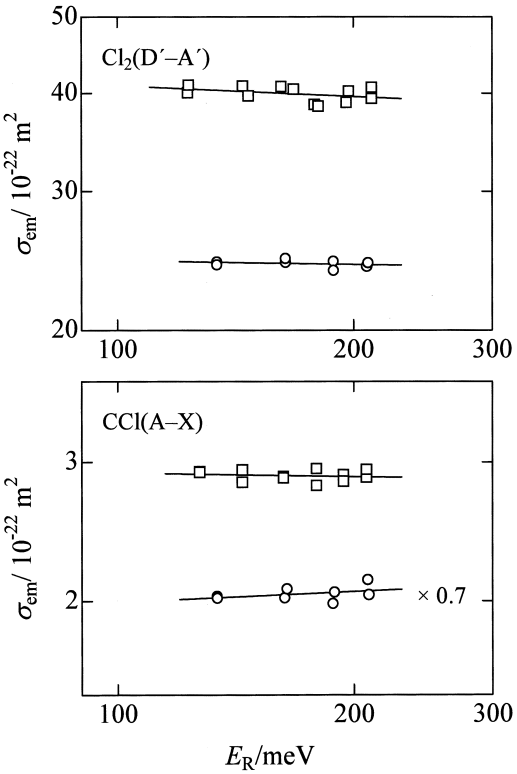

Fig. 2. The $\log\sigma_{em}(E_R)$ vs $\log(E_R)$ plots for the $Cl_2(D'–A')$ and CCl(A–X) emissions produced by collisions of He(2^3S) with $CHCl_3$ (□) and CCl_4 (○).

the orbiting cross section is represented by[9]

$$\sigma(E_R) \propto E_R^{-2/s}. \tag{11}$$

Thus, the negative dependence implies that an attractive potential between He(2^3S) and the target governs the formation of the fragments, while the positive dependence on the collision energy indicates that the interaction potential is repulsive, as discuss in later. The leading term of the attractive potential can be regarded as the type $s = 6$ for collisions of He(2^3S) with chloromethanes, but no correlation was found for the C_6 coefficient with the total σ_{em} or the σ_{em}^i. Higher order terms should be effective for the formation of excited fragments.

Figure 2 shows $\log\sigma_{em}(E_R)$ vs $\log(E_R)$ plots for the $Cl_2(D'–$

Table 3. Slope m Determined from $\log\sigma_{em}(E_R)$ vs $\log E_R$ Plots for the $Cl_2(D'–A')$ and CCl(A–X) Emissions from $CHCl_3$ and CCl_4

Target	E_R/meV	Emission	m
$CHCl_3$	123–210	$Cl_2(D'–A')$	-0.05 ± 0.06
		CCl(A–X)	-0.02 ± 0.05
CCl_4	134–210	$Cl_2(D'–A')$	-0.02 ± 0.06
		CCl(A–X)	0.04 ± 0.05

A′) and CCl(A–X) bands from $CHCl_3$ and CCl_4, and Table 3 lists the values of the slope m of the $\log\sigma_{em}(E_R)$ vs $\log(E_R)$ plots. Although we do not mention a quantitative comparison on the slope parameter m, because of the broad kinetic energy distribution of the He* beam, the qualitative features on the energy dependence seem to be clear. The σ_{em}'s for both bands are independent of the collision energy within the experimental uncertainty. Nevertheless, the m value for the $Cl_2(D'–A')$ band from $CHCl_3$ seems to be slightly negative, while that for the CCl(A–X) band from CCl_4 seem to be slightly positive. These results indicate that the effective potential between He(2^3S) and $CHCl_3$ or CCl_4 leading to $Cl_2(D')$ is either slightly attractive or nearly zero. This consideration is consistent with the conclusion that higher order interactions are dominant; the $|m|$ value decreases with increasing s in Eq. 10. We did not measure the dependence for CCl_2F_2, CCl_3F, and $CBrCl_3$ because of overlapping with other emissions.

Figures 3 and 4 show the potential-energy curves $V^*(R)$ for $CHCl_3$–He*(Li) and CCl_4–He*(Li), respectively, obtained from a model potential calculation; R is the distance between the Li atom and the C or Cl atom of the targets, when the Li atom approaches along several directions. For all cases the nuclear positions of $CHCl_3$ or CCl_4 were fixed at the experimental geometry.[30] This means that these curves correspond to the potential between the target and a fast He*(Li); the geometry of the target is frozen in the collision. In a collision with a slow He*(Li), the geometry of the target can be adequately relaxing during the collision. This effect on the interaction potential will appear as a downward deformation of the curve. Nevertheless, the deformation for rigid molecules is known to be negligible.[31]

The potential for $CHCl_3$–He*(Li) shows a shallow well depth of 10–20 meV around $R = 0.5$ nm, as shown in Fig. 3, when He*(Li) approaches the C atom. Similar depths are found when He*(Li) approaches the Cl atom along directions perpendicular to the molecular axis, whereas the well depth almost disappears when He*(Li) approaches the Cl atom along the molecular axis. Nevertheless, the anisotropy of the interaction potential is not so apparent. The potential for CCl_4–He*(Li) shows a shallow well depth of 10–17 meV, as shown in Fig. 4, when He*(Li) approaches the C or Cl atom along any direction. The prediction of a shallow well depth for the potentials for $CHCl_3$–He*(Li) and CCl_4–He*(Li) are consistent with either the independence or the slightly negative dependence of σ_{em} for the $Cl_2(D'–A')$ band on the collision energy.

Formation Mechanism of CCl(A) and $Cl_2(D')$. Dissociations resulting from the collisions of He(2^3S) with chloromethanes may be understood by either the harpoon model or the electron exchange model on the assumption that the entrance channel mainly governs the feature for the formation of excited fragments, and thus interactions in the exit channel have a minor effect on the feature.

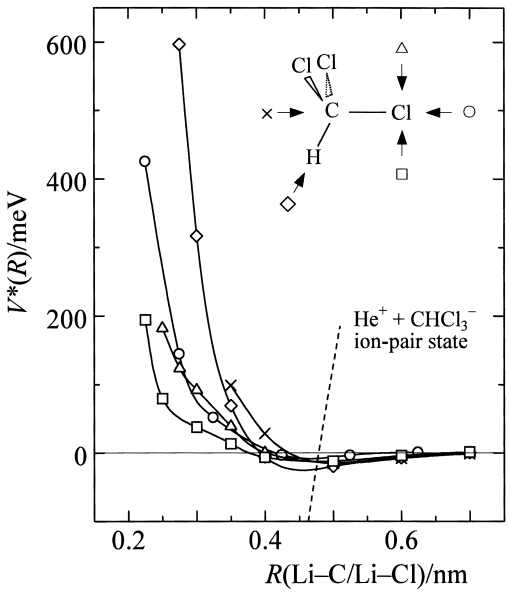

Fig. 3. Model potential curves $V^*(R)$ for $CHCl_3$–He*(Li) as function of the Li–C or Li–Cl distance calculated by MP2/6-31++G**.

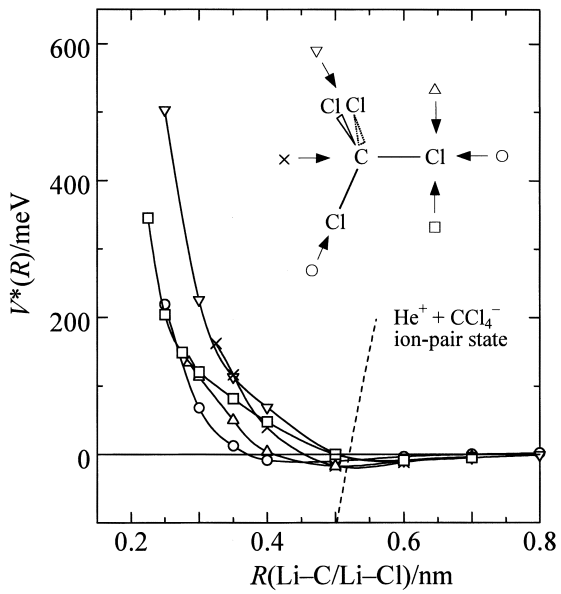

Fig. 4. Same as Fig. 3 but for CCl_4–He*(Li).

Figure 5 shows a correlation of σ^i_{em} with the $I(He^*) - E_a(M)$ value, where $I(He^*)$ is the ionization potential of He(2^3S) and $E_a(M)$ is the electron affinity of the target molecule (M);[32] no data is available for $CBrCl_3$. A pretty good correlation is found and the negative slope can be explained by the following model. The $I(He^*) - E_a(M)$ value corresponds the potential energy for the $He^+ + M^-$ system. The $He^+ + M^-$ curve, which is shown schematically in Figs. 3 and 4 shifts to the downside with increasing $E_a(M)$ and the crossing point (R_x)

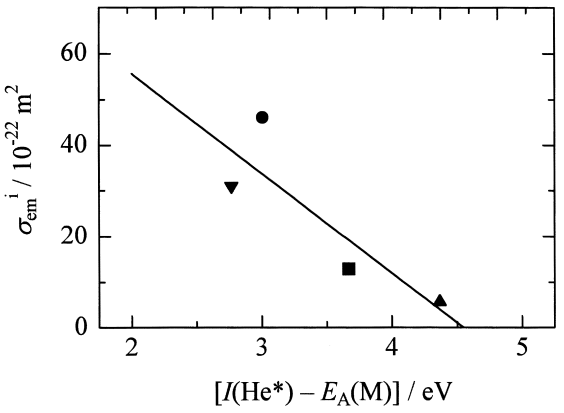

Fig. 5. Plot of σ_{em}^{i} vs the $I(He^*) - E_a(M)$ value; $CHCl_3$ (●), CCl_2F_2 (▲), CCl_3F (■), CCl_4 (▼), $CBrCl_3$ (◆).

between the He^* + M curve and the $He^+ + M^-$ curve then moves to the outer side; electron transfer can occur at R_x in the harpoon mechanism. The cross section for transfer to the $He^+ + M^-$ curve increases with R_x, and thus the correlation of the cross section with the $I(He^*) - E_a(M)$ value shows a negative slope. This consideration suggests that the harpoon mechanism can explain the formation of ion-pair states as an initial step. The potential curve correlating with the formation of the second group of emitters may cross with the $He^+ + M^-$ curve. The smallness of σ_{em}^{i}'s for chloromethanes, however, may be inconsistent with the harpoon model. Nevertheless, this discrepancy can be explained by the facts that the main decay channel should be Penning ionization. Moreover, many dissociation channels that do not emit photons are energetically possible. The branching in the exit channel is probably determined by subsequent short-range interactions during the collision process. Although we need to characterize the short-range interactions for fully understanding the branching process, the fairly good correlation shown in Fig. 5 indicates that the transition probability from the $He^+ + M^-$ curve to the curves correlating to formation of $Cl_2(D')$ is roughly equal among these chloromethanes.

A plot of the sum of σ_{em}'s for the first group of emitters against the $I(He^*) - E_a(M)$ value was found to have a positive slope. This result indicates that the harpoon mechanism cannot explain the formation of the first group of emitters. Thus, we prefer the electron exchange mechanism for the formation of the first group. The dependence of σ_{em} for the CCl(A–X) band on the collision energy can provide useful information on the interaction potential correlating to the formation of the first group of emitters. The slopes for the CCl(A–X) band indicate that the effective potentials between He(2^3S) and $CHCl_3$ or CCl_4 are nearly zero, or slightly repulsive. In the electron-exchange mechanism, the electron transfer is expected to occur near the van der Waals distance of He(2^3S) with the target; thus, the positive m value reflects the steepness of the repulsive part of $V^*(R)$.[13] The repulsive parts of $V^*(R)$ for $CHCl_3$–He^*(Li) and CCl_4–He^*(Li) are rather gentle in the 0–200 meV region, except for the case that He^* approaches the C atom along the C–H axis of $CHCl_3$. When the repulsive part is gentle, the classical turning point easily moves to the inner side with increasing the collision energy, and then the slope (m) becomes large.[33] This consideration indicates that the electron exchange to the dissociation channel correlating to the formation of CCl(A) seems to occur at a relatively large distance, where the repulsive part of the interaction potential is not so important.

Conclusions

We have studied the formation of electronically excited neutral fragments by the collision of He(2^3S) with chloromethanes. The total σ_{em}'s in the 190–600 nm region is estimated to be about 1% of the quenching cross sections of He(2^3S). The collision energy dependences of σ_{em} for the $Cl_2(D'–A')$ band are nearly zero, or slightly negative. Fairly good correlations are found for the sum of σ_{em}'s for the ion-pair states with the electron affinity of the targets. These results strongly indicate that the formation of ion-pair states by collisions of He(2^3S) with chloromethanes is governed by the harpoon mechanism despite the smallness of their σ_{em}'s. Further, the electron exchange mechanism probably governs the formation of the first group of emitters (H, CH, CF, and CCl fragments). These conclusions are consistent with the model potentials calculated for $CHCl_3$–He^*(Li) and CCl_4–He^*(Li).

This work was partly supported by a Grand-in-Aid for Scientific Research from the Ministry of Education, Science, Sports and Culture.

References

1 a) A. Fontijn, *Prog. React. Kinet.*, **6**, 75 (1971). b) D. H. Stedman and D. W. Setser, *Prog. React. Kinet.*, **6**, 193 (1971).

2 D. J. Wren, D. W. Setser, and J. K. Ku, *J. Phys. Chem.*, **86**, 284 (1982).

3 J. Guo, Y. Gu, C. Liu, Y. Yin, D. Cao, and D. Cai, *Chem. Phys. Lett.*, **169**, 432 (1990).

4 K. T. Wu, C. Mendis, A. Abrahim, and R. Oldmixon, *Chem. Phys. Lett.*, **210**, 118 (1993).

5 Q. Li, C. Chen, X. Ma, X. Li, and G. Shen, *Chem. Phys. Lett.*, **224**, 225 (1994).

6 M. Tsuji, T. Mizuguchi, K. Shinohara, and Y. Nishimura, *Can. J. Phys.*, **61**, 838 (1983).

7 M. Tsuji, M. Furusawa, T. Mizuguchi, T. Muraoka, and Y. Nishimura, *J. Chem. Phys.*, **97**, 245 (1992).

8 a) H. Hotop and A. Niehaus, *Z. Phys.*, **228**, 68 (1969). b) H. Hotop and A. Niehaus, *Chem. Phys. Lett.*, **8**, 497 (1971). c) W. H. Miller, *J. Chem. Phys.*, **52**, 3563 (1970).

9 A. Niehaus, *Adv. Chem. Phys.*, **45**, 399 (1981), and references cited therein.

10 R. L. Platzman, *The Vortex*, **23**, 372 (1962).

11 I. Tokue, T. Kudo, and Y. Ito, *Chem. Phys. Lett.*, **199**, 435 (1992).

12 I. Tokue, Y. Sakai, and K. Yamasaki, *J. Chem. Phys.*, **106**, 4491 (1997).

13 K. Ohno, T. Takami, K. Mitsuke, and T. Ishida, *J. Chem. Phys.*, **94**, 2675 (1991).

14 R. A. Sanders, A. N. Schweid, M. Weiss, and E. E. Muschlitz Jr., *J. Chem. Phys.*, **65**, 2700 (1976).

15 F. J. Comes and F. Speier, *Chem. Phys. Lett.*, **4**, 13 (1969).

16 a) H. Hotop, *Radiat. Res.*, **59**, 379 (1974). b) H. Haberland, Y. T. Lee, and P. E. Siska, *Adv. Chem. Phys.*, **45**, 487

(1981).

17 K. Ohno and S. Sunada, *Proc. Indian Acad. Sci.*, **106**, 327 (1994).

18 M. J. Frisch, G. W. Trucks, H. B. Schlegel, P. M. W. Gill, B. G. Johnson, M. A. Robb, J. R. Cheeseman, T. Keith, G. A. Petersson, J. A. Montgomery, K. Raghavachari, M. A. Al-Laham, V. G. Zakrzewski, J. V. Ortiz, J. B. Foresman, C. Y. Peng, P. Y. Ayala, W. Chen, M. W. Wong, J. L. Andres, E. S. Replogle, R. Gomperts, R. L. Martin, D. J. Fox, J. S. Binkley, D. J. Defrees, J. Baker, J. P. Stewart, M. Head-Gordon, C. Gonzalez, and J. A. Pople, "Gaussian 94, Revision B.2," Gaussian Inc., Pittsburgh PA, (1995).

19 M. Kusakabe, Y. Ito, and I. Tokue, *Chem. Phys.*, **170**, 243 (1993), and references cited therein.

20 M. Diegelman, K. Hohla, F. Rebentrost, and K. L. Kompa, *J. Chem. Phys.*, **76**, 1233 (1982).

21 P. C. Tellinghuisen, B. Guo, D. K. Chakraborty, and J. Tellinghuisen, *J. Mol. Spectrosc.*, **128**, 268 (1988).

22 I. Tokue, T. Honda, and Y. Ito, *Chem. Phys.*, **140**, 157 (1990).

23 E. B. Andrews and R. F. Barrow, *Proc. Phys. Soc. A*, **64**, 481 (1951).

24 T. Ueno, A. Yokoyama, S. Takao, and Y. Hatano, *Chem. Phys.*, **45**, 261 (1980).

25 J. P. Riola, J. S. Howard, R. D. Rundel, and R. F. Stebbings, *J. Phys. B*, **2**, 376 (1974).

26 A. L. Schmeltekopf and F. C. Fehsenfeld, *J. Chem. Phys.*, **53**, 3173 (1970).

27 a) D. D. Wagman, W. H. Evans, V. B. Parker, R. H. Schumm, I. Halow, S. M. Bailey, K. L. Churney, and R. L. Nuttall, *J. Phys. Chem. Ref. Data*, **11**, Suppl. No. 2 (1982). b) M. W. Chase Jr., C. A. Davies, J. R. Downey Jr., D. J. Frurip, R. A. McDonald, and A. N. Syverud, *J. Phys. Chem. Ref. Data*, **14**, Suppl. No. 1 (1985). c) S. G. Lias, Z. Karpas, and J. F. Liebman, *J. Am. Chem. Soc.*, **107**, 6089 (1985).

28 K. P. Huber and G. Herzberg, "Molecular Spectra and Molecular Structure, Vol. 4, Constants of Diatomic Molecules," Van Nostrand–Reinhold, New York, (1979).

29 D. A. Predmore, A. M. Murray, and M. D. Harmony, *Chem. Phys. Lett.*, **110**, 173 (1984).

30 a) Y. Morino, Y. Nakamura, and T. Iijima, *J. Chem. Phys.*, **32**, 643 (1960). b) M. Jen and D. R. Lide, *J. Chem. Phys.*, **36**, 2525 (1962).

31 T. Pasinszki, H. Yamakado, and K. Ohno, *J. Phys. Chem.*, **99**, 14678 (1995).

32 A. A. Christodoulides, D. L. McCorkle, and L. G. Christophorou, in "Electron–Molecule Interactions and Their Applications Vol. 2," ed by L. G. Christophorou, Academic press, Orlando (1984), Table 2.

33 T. Takami, K. Mitsuke, and K. Ohno, *J. Chem. Phys.*, **95**, 918 (1991).